arXiv:2404.07050v1 [cond-mat.stat-mech] 10 Apr 2024

Three-dimensional $\mathbb{Z}_2$-gauge N-vector models

Claudio Bonati,[1] Andrea Pelissetto,[2] and Ettore Vicari[3]

[1] *Dipartimento di Fisica dell'Università di Pisa and INFN Sezione di Pisa, Largo Pontecorvo 3, I-56127 Pisa, Italy*
[2] *Dipartimento di Fisica dell'Università di Roma Sapienza and INFN Sezione di Roma I, I-00185 Roma, Italy*
[3] *Dipartimento di Fisica dell'Università di Pisa, Largo Pontecorvo 3, I-56127 Pisa, Italy*

(Dated: April 11, 2024)

We study the phase diagram and critical behaviors of three-dimensional lattice $\mathbb{Z}_2$-gauge N-vector models, in which an N-component real field is minimally coupled with a $\mathbb{Z}_2$-gauge link variables. These models are invariant under global $\mathrm{O}(N)$ and local $\mathbb{Z}_2$ transformations. They present three phases characterized by the spontaneous breaking of the global $\mathrm{O}(N)$ symmetry and by the different topological properties of the $\mathbb{Z}_2$-gauge correlations. We address the nature of the three transition lines separating the three phases. The theoretical predictions are supported by numerical finite-size scaling analyses of Monte Carlo data for the $N = 2$ model. In this case, continuous transitions can be observed along both transition lines where the spins order, in the regime of small and large inverse gauge coupling K. Even though these continuous transitions belong to the same XY universality class, their critical modes turn out to be different. When the gauge variables are disordered (small K), the relevant order-parameter field is a gauge-invariant bilinear combination of the vector field. On the other hand, when the gauge variables are ordered (large K), the order-parameter field is the gauge-dependent N-vector field, whose critical behavior can only be probed by using a stochastic gauge fixing that reduces the gauge freedom.

I. INTRODUCTION

Gauge symmetries and Higgs phenomena are key features of theories describing high-energy particle physics [1] and collective phenomena in condensed-matter physics [2–5]. In both contexts, it is crucial to have a solid understanding of the interplay between global and gauge symmetries, and, in particular, of the role that local gauge symmetries play in determining the phase structure of a model, the nature of its different phases and of its quantum and thermal transitions. Several lattice Abelian and non-Abelian gauge models have been considered, with the purpose of identifying the possible universality classes of the continuous transitions, see, e.g., Refs. [5–86] for a partial selection of references. They provide examples of topological transitions, which are driven by extended charged excitations with no local order parameter, or by a nontrivial interplay between long-range scalar fluctuations and nonlocal topological gauge modes.

In this paper we discuss the phase diagram and critical behavior of three-dimensional (3D) lattice $\mathbb{Z}_2$-gauge N-vector models, obtained by minimally coupling N-component real variables with $\mathbb{Z}_2$-gauge variables. They are interesting paradigmatic models with different phases characterized by the spontaneous breaking of the global $\mathrm{O}(N)$ symmetry and by the different topological properties of the $\mathbb{Z}_2$-gauge correlations, see, e.g., Refs. [5, 9]. Moreover, they are relevant for transitions in nematic liquid crystal, see, e.g., Refs. [19, 56], and for systems with fractionalized quantum numbers, see, e.g., Ref. [25, 26].

The phase diagram of the 3D $\mathbb{Z}_2$-gauge N-vector model presents three phases distinguished by the order/disorder of the spin correlations and the order/disorder of the $\mathbb{Z}_2$-gauge correlations. A sketch of the phase diagram for $N \geq 2$ is shown in Fig. 1. There are two spin-disordered phases separated by a topological $\mathbb{Z}_2$-gauge transition, and one spin-ordered phase with topologically trivial gauge correlations. These phases are separated by three transition lines, whose nature crucially depends on N, with the exception of the purely topological transition between the spin-disordered phases, which belongs to the $\mathbb{Z}_2$-gauge universality class [5, 6, 9] for any N (obviously the presence of first order transitions cannot be excluded by universality arguments). For $N \geq 3$ the DD-O transitions are expected to be first order, while along the DO-O transition line the system undergoes continuous transitions belonging to the $\mathrm{O}(N)$ vector universality class. Note, however, that along the DO-O transition line there are apparently no critical vector correlations, be-

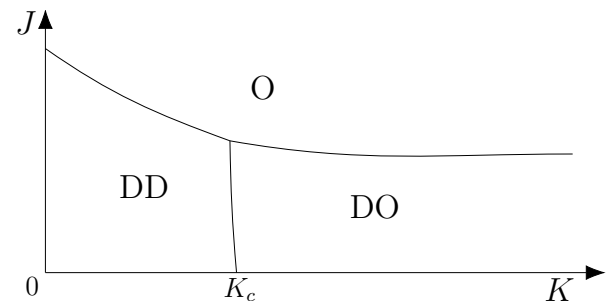

FIG. 1: Sketch of the phase diagram of the 3D $\mathbb{Z}_2$-gauge N-vector model with $N \geq 2$ in the space of the Hamiltonian parameters K and J, cf. Eq. (2), where K is the inverse gauge coupling and J is the spin hopping parameter. There are two spin-disordered phases for small J: a small-K phase, in which both spin and $\mathbb{Z}_2$-gauge variables are disordered (we indicate it by DD), and a large-K phase, in which the $\mathbb{Z}_2$-gauge variables order (we indicate it by DO). For large J there is a single phase, in which both spins and gauge variables are ordered (we indicate it by O).

cause of the $\mathbb{Z}_2$-gauge invariance. To identify a vector critical field, it is necessary to reduce the gauge freedom, by performing an appropriate gauge fixing. We use the stochastic gauge fixing outlined in Ref. [87].

Unlike models with $N \geq 3$, the model with $N = 2$ can develop continuous transitions along all three transition lines. In particular, the DD-O and DO-O continuous transitions (see Fig. 1) between the spin-disordered phases and the spin-ordered one are both expected to belong to the XY universality class. However, this does not imply that the relevant critical modes are the same. Indeed, as we shall see, the correlations of the gauge-invariant operators have a different critical behavior along the DD-O and DO-O transition lines.

To numerically check the theoretical predictions, we report Monte Carlo (MC) simulations of the $N = 2$ model in different regions of its phase diagram. A finite-size scaling (FSS) analysis of the numerical data confirms the general picture. The system undergoes continuous transitions along all three transition lines, except possibly sufficiently close to the meeting point of the transition lines where the transitions may turn into first-order ones. Along the DD-O and DO-O transition lines continuous transitions belong to the XY universality class. However, while the order parameter for the DD-O transitions is a gauge-invariant variable, the order parameter along the DO-O transition line can be identified with the non-gauge-invariant spin variable, after an appropriate gauge fixing procedure (without fixing the gauge, the correlation functions of the vector variables trivially vanish).

The paper is organized as follows. In Sec. II we introduce the 3D $\mathbb{Z}_2$-gauge N-vector models. The phase diagram and nature of the transition lines for $N \geq 2$ are discussed in Sec. III. In Sec. IV we present our numerical results for $N = 2$. In Sec. V we focus on the transitions at the meeting point of the three transition lines separating the different phases. In Sec. VI we present results obtained by the stochastic gauge fixing put forward in Ref. [87], which allows us to observe critical vector correlations along the DO-O line. Finally, in Sec. VII we summarize and draw our conclusions.

II. THE $\mathbb{Z}_2$-GAUGE N-VECTOR MODELS

We consider lattice N-vector models with local $\mathbb{Z}_2$ gauge invariance, defined on a 3D cubic lattice of linear size L with periodic boundary conditions. The system variables are unit-length N-component real vectors $\boldsymbol{s}_{\boldsymbol{x}}$ (i. e., $\boldsymbol{s}_{\boldsymbol{x}} \in \mathbb{R}^N$ and $\boldsymbol{s}_{\boldsymbol{x}} \cdot \boldsymbol{s}_{\boldsymbol{x}} = 1$) defined on the lattice sites, and $\mathbb{Z}_2$ spins $\sigma_{\boldsymbol{x},\mu} = \pm 1$ defined on the bonds ($\sigma_{\boldsymbol{x},\mu}$ is associated with the bond starting from site $\boldsymbol{x}$ in the positive μ direction, $\mu = 1, 2, 3$). The partition function reads

$$Z = \sum_{\{\boldsymbol{s},\sigma\}} e^{-H(J,K)/T}, \tag{1}$$

where $H(J, K)$ is the lattice Hamiltonian defined by

$$H(J, K) = H_{\boldsymbol{s}}(J) + H_\sigma(K), \tag{2}$$

where

$$H_{\boldsymbol{s}}(J) = -JN \sum_{\boldsymbol{x},\mu} \sigma_{\boldsymbol{x},\mu}\, \boldsymbol{s}_{\boldsymbol{x}} \cdot \boldsymbol{s}_{\boldsymbol{x}+\hat{\mu}}, \tag{3}$$

$$H_\sigma(K) = -K \sum_{\boldsymbol{x},\mu>\nu} \sigma_{\boldsymbol{x},\mu}\, \sigma_{\boldsymbol{x}+\hat{\mu},\nu}\, \sigma_{\boldsymbol{x}+\hat{\nu},\mu}\, \sigma_{\boldsymbol{x},\nu}. \tag{4}$$

By measuring energies in units of the temperature T, we can formally set $T = 1$ in Eq. (1). The Hamiltonian (2) is invariant under global O(N) transformations acting on the spin variables $\boldsymbol{s}_{\boldsymbol{x}}$, and under local $\mathbb{Z}_2$ gauge transformations, $\boldsymbol{s}_{\boldsymbol{x}} \to w_{\boldsymbol{x}} \boldsymbol{s}_{\boldsymbol{x}}$ and $\sigma_{\boldsymbol{x},\nu} \to w_{\boldsymbol{x}} \sigma_{\boldsymbol{x},\nu} w_{\boldsymbol{x}+\hat{\nu}}$ with $w_{\boldsymbol{x}} = \pm 1$. For $N = 1$ the spin variables take the integer values $s_{\boldsymbol{x}} = \pm 1$, and the model corresponds to the so-called $\mathbb{Z}_2$ gauge Higgs model [6, 9, 10].

The critical behavior at the phase transitions can be determined by analyzing the FSS behavior of gauge-invariant correlation functions. For this purpose, for $N \geq 2$, we consider the spin-two bilinear operator

$$Q^{ab}_{\boldsymbol{x}} = s^a_{\boldsymbol{x}} s^b_{\boldsymbol{x}} - \frac{1}{N} \delta^{ab}, \tag{5}$$

and its correlation function

$$G(\boldsymbol{x}, \boldsymbol{y}) = \langle \mathrm{Tr}\, Q_{\boldsymbol{x}} Q_{\boldsymbol{y}} \rangle. \tag{6}$$

The corresponding susceptibility χ and second-moment correlation length ξ are defined as

$$\chi \equiv \widetilde{G}(\boldsymbol{0}), \quad \xi^2 \equiv \frac{1}{4 \sin^2(\pi/L)} \frac{\widetilde{G}(\boldsymbol{0}) - \widetilde{G}(\boldsymbol{p}_m)}{\widetilde{G}(\boldsymbol{p}_m)}, \tag{7}$$

where $\widetilde{G}(\boldsymbol{p}) = \sum_{\boldsymbol{x}} e^{i\boldsymbol{p}\cdot\boldsymbol{x}} G(\boldsymbol{x})$ and $\boldsymbol{p}_m = (2\pi/L, 0, 0)$. We also consider renormalization-group (RG) invariant quantities, whose scaling behavior does not depend on any nonuniversal normalization, such as the ratio

$$R \equiv \xi/L, \tag{8}$$

and the Binder parameter defined as

$$U = \frac{\langle m_2^2 \rangle}{\langle m_2 \rangle^2}, \qquad m_2 = \frac{1}{L^d} \sum_{\boldsymbol{x},\boldsymbol{y}} \mathrm{Tr}\, Q_{\boldsymbol{x}} Q_{\boldsymbol{y}}. \tag{9}$$

III. THE PHASE DIAGRAM

The phase diagram of the $\mathbb{Z}_2$ Higgs model, corresponding to the model (2) with $N = 1$, has already been thoroughly investigated, see, e.g., Refs. [46, 74, 76]. Its phase diagram is reported in Fig. 2. In the following we focus on the multicomponent cases, $N \geq 2$. To understand their phase diagram, we first consider some limiting cases, corresponding to simpler models whose thermodynamic behavior is already known. Their transition points are then expected to be the starting points of transition lines, which separate the different phases of the model with Hamiltonian (2).

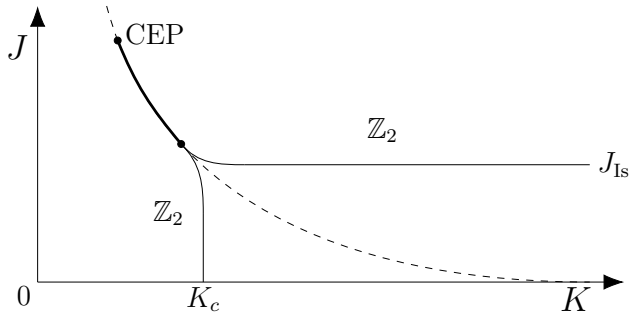

FIG. 2: Sketch of the phase diagram of the 3D $\mathbb{Z}_2$ gauge Higgs model, see, e.g., Refs. [46, 74, 76]. The dashed line is the self-dual line, the thick line is a finite stretch of the self-dual line corresponding to first-order transitions. The two lines labelled "$\mathbb{Z}_2$" are related by duality, and correspond to Ising continuous transitions. They end at $[J = J_{\rm Is} \approx 0.221655, K = \infty]$ and at $[J = 0, K = K_{\mathbb{Z}_2} \approx 0.761413]$. The three lines meet at a multicritical point [46, 74, 76, 88, 89] at $[K_\star = 0.7525(1), J_\star \approx 0.22578(5)]$. The corresponding multicritical behavior is controlled by the multicritical XY fixed point [76, 89, 90]. The second endpoint (CEP) of the first-order transition line, at $[K \approx 0.688, J \approx 0.258]$, is expected to be an Ising critical endpoint.

A. The transition line starting from $J = 0$

For $J = 0$ the model reduces to the $\mathbb{Z}_2$ gauge model [6] for any N. Therefore, there is a continuous topological phase transition along the line $J = 0$, which is that of the $\mathbb{Z}_2$ gauge model, at [91, 92] $K_{\mathbb{Z}_2} = 0.761413292(11)$, separating a confined phase at small K from a deconfined phase at large K. This critical point is expected to be the starting point of a transition line, which separates two phases with different topological $\mathbb{Z}_2$ gauge properties [9]: the gauge modes are disordered for small K, ordered in the oppostite case (see, e.g., Ref. [5]). Both phases are disordered with respect to the spin variables.

Since the spin variables are not critical for sufficiently small values of J, they can be integrated out. At leading order in J, one obtains again the $\mathbb{Z}_2$ gauge model [6, 9, 10, 19], with a renormalized gauge coupling K, i.e., $K \to K(J) = K + NJ^4$. This result indicates that the transition line starting from $(J = 0, K = K_{\mathbb{Z}_2})$ bends toward small values of K, as

$$K_c(J) = K_{\mathbb{Z}_2} - NJ^4 + O(J^6). \tag{10}$$

The existence of such topological transition line should be limited to the region where the spin variables $\boldsymbol{s}_{\boldsymbol{x}}$ are disordered, therefore, for sufficiently small values of J.

We also mention that no phase transitions are expected in the opposite limit $J \to \infty$, where the spin and gauge variables order. In this limit, modulo gauge transformations, we can set $\boldsymbol{s}_x = \boldsymbol{e}$ and $\sigma_{\boldsymbol{x},\mu} = 1$, where $\boldsymbol{e}$ is a unit vector.

B. The transition line starting from $K = 0$

For $K = 0$, the $\mathbb{Z}_2$ gauge variables can be easily integrated out, obtaining a lattice formulation of the so-called RP^{N-1} model, whose Hamiltonian is

$$\begin{aligned} H_{K=0} &= -\sum_{\boldsymbol{x},\mu} \ln\left[2\cosh(JN\, \boldsymbol{s}_{\boldsymbol{x}} \cdot \boldsymbol{s}_{\boldsymbol{x}+\hat\mu})\right] \\ &= -\sum_{\boldsymbol{x},\mu} \left[\ln 2 + \frac{J^2N^2}{2} |\boldsymbol{s}_{\boldsymbol{x}} \cdot \boldsymbol{s}_{\boldsymbol{x}+\hat\mu}|^2 + O(J^4)\right]. \end{aligned} \tag{11}$$

Like the standard RP^{N-1} model with Hamiltonian $H_{RP} = -J' \sum_{\boldsymbol{x},\mu} |\boldsymbol{s}_{\boldsymbol{x}} \cdot \boldsymbol{s}_{\boldsymbol{x}+\hat\mu}|^2$, the variant model with Hamiltonian (11) is expected to undergo a phase transition for any $N \geq 2$ (no phase transitions occur at $K = 0$ for $N = 1$, see Fig. 2, because the Hamiltonian H_{RP} is trivial in this case).

Since the gauge modes are not critical, the nature of the phase transitions in RP^{N-1} models can be inferred by means of a standard Landau-Ginzburg-Wilson (LGW) argument. We consider a field Φ^{ab}, which is a symmetric traceless matrix obtained by coarse-graining the order parameter (5), and the LGW Hamiltonian (see, e.g., Refs. [62, 63])

$$\begin{aligned} \mathcal{L}_{\rm LGW} &= {\rm Tr}(\partial_\mu \Phi)^2 + r\, {\rm Tr}\, \Phi^2 \\ &+ w\, {\rm tr}\, \Phi^3 + u\, ({\rm Tr}\, \Phi^2)^2 + v\, {\rm Tr}\, \Phi^4. \end{aligned} \tag{12}$$

For $N = 2$ the Lagrangian (12) is equivalent to that of the XY vector model (in particular, the Φ^3 term cancels). Thus, continuous transitions should belong to the XY universality class [93]. For larger values of N, the LGW approach predicts all transitions to be of first order, because of the presence of the Φ^3 term, see, e.g., Ref. [94].

A natural hypothesis is that a transition line starts from the transition point at $K = 0$, with the same critical behavior as for $K = 0$. Therefore, for small values of K we expect a continuous XY transition line for $N = 2$ and a first-order transition line for any $N \geq 3$.

C. The transition line starting from $K = \infty$

For $K \to \infty$, the plaquettes must take their maximum value, i.e.,

$$\Pi_{\boldsymbol{x},\mu\nu} = \sigma_{\boldsymbol{x},\mu}\, \sigma_{\boldsymbol{x}+\hat\mu,\nu}\, \sigma_{\boldsymbol{x}+\hat\nu,\mu}\, \sigma_{\boldsymbol{x},\nu} = 1. \tag{13}$$

Therefore, in infinite volume, modulo gauge transformations, we can set $\sigma_{\boldsymbol{x},\mu} = 1$. The Hamiltonian (2) coincides therefore with that of the standard lattice N-vector model without gauge variables. It follows that, for $K \to \infty$, the system undergoes a continuous transition at $J_c(K = \infty) = J_{c,{\rm O}(N)}$, belonging to the O($N$) vector universality class. Estimates of the critical point $J_{c,{\rm O}(N)}$ in N-vector models can be found in Refs. [95–101]. In

particular, $J_{c,\mathrm{O}(2)} = 0.22708234(9)$ for $N = 2$ [95], and $J_{c,\mathrm{O}(N)} = 0.252731...$ for $N \to \infty$ [101].

It is again natural to conjecture the existence of a transition line that starts from the O(N) transition point for $K \to \infty$. Along this line, for sufficiently large values of K, we expect transitions to belong to the O(N) universality class as for $K = \infty$. Indeed, if the probability that $\Pi_{\boldsymbol{x},\mu\nu} = -1$ is sufficiently small (as expected in the large-K and low-J phase), the nature of the transition should be the same as for $K = \infty$. The stability of the $K \to \infty$ O(N)-vector fixed point against gauge fluctuations is essentially related to the discrete nature of the gauge variables, whose fluctuations are suppressed in the topologically ordered phase. Note that, in the presence of continuous Abelian and non-Abelian gauge symmetries, gauge interactions destabilize the N-vector critical behavior observed for $K = \infty$, In this case, even for large values of K, transitions along the line that ends in the N-vector critical point for $K = \infty$, do not belong to the N-vector universality class and have a different nature, see, e.g., Refs. [66, 76, 80, 83, 84]

We remark that the prediction that the large-K transitions belong to the N-vector universality class is apparently in contradiction with what one would obtain from a naive application of the LGW approach. Indeed, in N-vector transitions the order parameter is the magnetization, i.e., the spin $\boldsymbol{s}_{\boldsymbol{x}}$. But, the spin is not gauge invariant, and indeed the vector correlation function $\langle \boldsymbol{s}_{\boldsymbol{x}} \cdot \boldsymbol{s}_{\boldsymbol{y}} \rangle$ vanishes for $\boldsymbol{x} \neq \boldsymbol{y}$. Only gauge-invariant operators are critical, the simplest one being the spin-two operator introduced in Eq. (5). Thus, in a naive application of the LGW approach, one would reason as in Sec. III B, obtaining the LGW Lagrangian (12), and therefore predicting the transition lines DD-O and DO-O to have the same nature. These conclusions contradict the arguments given above for the large-K transition line.

In the following, we will provide robust evidence that the large-K transitions belong to the O(N) vector universality class. This implies that the naive LGW argument is incorrect when applied to the DO-O transitions. Indeed, along this line, the order parameter turns out to be a vector field, like the standard N-vector models, although such vector order parameter cannot be directly identified in the $\mathbb{Z}_2$-gauge N-vector models, because of the gauge invariance. It emerges only once an appropriate gauge fixing is introduced, as discussed in Ref. [87]. Note that an appropriate gauge fixing is needed not only for finite values of K but also for $K = \infty$. Indeed, we obtain the N-vector Hamiltonian only if we fix the gauge so that $\sigma_{\boldsymbol{x},\mu} = 1$ on all links.

It is worth noting that, for $N = 2$, the LGW model with Lagrangian (12) predicts an XY critical behavior as the corresponding N-vector LGW theory. However, in the first case $Q^{ab}_{\boldsymbol{x}}$ behaves as a two-component vector field, while in the second case $Q^{ab}_{\boldsymbol{x}}$ is a spin-two operator. Thus, the critical behavior of $Q^{ab}_{\boldsymbol{x}}$ allows us to distinguish which is the appropriate LGW description of the transition. For $N \geq 3$ the LGW predictions are different. In particular, the theory with Lagrangian (12) predicts first-order transitions because of the cubic term. Even admitting the possibility that the cubic term somehow vanishes, as for antiferromagnetic RP^{N-1} models, the critical behavior would be different from the O(N)-vector one (see Ref. [63] for a RG analysis of the theory with Lagrangian (12) and $w = 0$).

D. The J-K phase diagram

To draw the phase diagram in the J-K parameter space of the N-component model, we make the natural hypothesis that the transitions identified along the lines $K = 0$, $K = \infty$, and $J = 0$ are the starting points of three transition lines that meet in a single point, as sketched in Fig. 1. These transition lines are the boundaries of three different phases. For small values of J we expect two phases in which the spin variables are disordered. For small K also the gauge degrees of freedom are disordered—we name this phase disordered-disordered (DD) phase. For large K, instead, gauge variables are topologically ordered—this is the disordered-ordered (DO) phase. For large J there is instead a single phase, in which both spin and gauge variables are ordered—we name it ordered (O) phase. In this phase the bilinear spin-two operator $Q^{ab}_{\boldsymbol{x}}$ condenses.

As already discussed, for sufficiently small K, the DD-O transitions should have the same nature as the RP^{N-1} transition along the $K = 0$ line. The corresponding critical behavior id therefore controlled by the LGW theory (12). Instead, for sufficiently large values of K along the DO-O transition line, we expect transitions to belong to the O(N) vector universality class. Spin variables should not play any role along the DD-DO transition, which should have the same topological nature as the transition in the pure $\mathbb{Z}_2$ gauge theory.

E. Meeting point of the transition lines

The three transition lines are expected to eventually meet at one point $[K_\star, J_\star]$ of the phase diagram. Eq. (10) suggests that $K_\star \lesssim K_{\mathbb{Z}_2} \approx 0.761$ at least for small N. Indeed, if we assume that the DD-O line $J = J_c(K)$ is weakly dependent on K, as it occurs in the $\mathbb{Z}_2$ Higgs model whose phase diagram in shown in Fig. 2, the correction term in Eq. (10) is small (of the order of $N J^4_{c,\mathrm{O}(N)}$, with $J_{c,\mathrm{O}(N)} \approx 0.2$). . This is consistent with the results reported in Sec. V, where we argue that $K_\star \approx 0.75$ for $N = 2$.

At the meeting point the system may develop a multicritical behavior if some of the transition lines are continuous at the meeting point, as it happens in the $\mathbb{Z}_2$ gauge Higgs model (see Fig. 2). Alternatively, if all transition lines are of first order, the meeting point corresponds to a first-order transition. We shall return to this point in Sec. V.

F. Phase behavior for $N = 2$

We now focus on the two-component model, which is particularly interesting because it is the only case in which continuous transitions may occur along all three transition lines. In particular, on the basis of the above discussion, the continuous transitions along the DD-O and DO-O lines are expected to both belong to the XY universality class. However, as discussed in Sec. III C, the nature of the transitions along the two lines is not the same and this shows up in the different critical behavior of the operator $Q^{ab}_{\boldsymbol{x}}$ defined in Eq. (5).

To characterize continuous transitions along the DD-O and DO-O lines, we fix K and vary the parameter J. Close to the transition, the correlation function $G(\boldsymbol{x}, \boldsymbol{y})$ defined in Eq. (6) is expected to show the asymptotic FSS behavior (we assume that the boundary conditions preserve translation invariance)

$$G(\boldsymbol{x}_1, \boldsymbol{x}_2, J, L) \approx L^{-2Y_Q} [\mathcal{G}(\boldsymbol{X}, W) + O(L^{-\omega})], \quad (14)$$

$$\boldsymbol{X} = (\boldsymbol{x}_1 - \boldsymbol{x}_2)/L, \quad W = (J - J_c)L^{1/\nu}, \quad (15)$$

where Y_Q is the RG dimension of the operator $Q^{ab}_{\boldsymbol{x}}$. Since both DD-O and DO-O transitions belong to the XY universality class, we have $\nu = \nu_{XY} = 0.6717(1)$ and $\omega = \omega_{XY} = 0.789(4)$ [95, 102–105]. However, the RG dimension Y_Q differs along the DD-O and DO-O transition lines.

Along the DD-O line, an effective description is provided by the LGW model with Lagrangian (12). In this case the coarse-grained field Φ^{ab} is equivalent to an O(2) vector field. This implies that the RG dimension Y_Q of $Q^{ab}_{\boldsymbol{x}}$ coincides with the RG dimension $Y_{V,XY}$ of the vector field in the standard XY model. Thus, at continuous transitions along the DD-O line, we have

$$Y_Q = Y_{V,XY} = \frac{d - 2 + \eta_{XY}}{2} = 0.519088(22) \quad (16)$$

where we used the precise estimate [105] $\eta_{XY} = 0.038176(44)$.

On the other hand, the continuous transitions along the DO-O transition line are expected to belong to the N-vector universality class. Therefore, the bilinear operator Q corresponds to the tensor spin-two operator in the XY model, whose RG dimension $Y_{T,XY}$ has been computed by various methods, see Refs. [105–108]. Therefore, we expect

$$Y_Q = Y_{T,XY} = 1.23629(11) \quad (17)$$

at the continuous transitions along the DO-O line.

As a consequence of the above results, the susceptibility defined in Eq. (7) has a substantially different dependence on the size of the system at critical points along the two lines, a difference that can be easily detected in FSS analyses. Since χ behaves as

$$\chi \approx L^{d-2Y_Q} \mathcal{A}(W) \quad (18)$$

K	$J_c(K)$	type	Y_Q
0	0.79305(7)	XY	$Y_{V,XY}$
0.5	0.37118(2)	XY	$Y_{V,XY}$
0.7	0.2520(3)	$1^{\rm st}$-order	
0.8	0.229(1)	XY	$Y_{T,XY}$
1	0.22729(3)	XY	$Y_{T,XY}$
∞	0.22708234(9)	XY	$Y_{T,XY}$

TABLE I: Results obtained for $N = 2$, varying J across the DD-O and DO-O transition lines for fixed values of K. We report the critical point $J_c(K)$ (for $K \to \infty$ we quote the estimate of the XY critical point reported in Ref. [95]), the transition type, and, if the transition is continuous, the value of the RG dimension Y_Q of the gauge-invariant operator $Q^{ab}_{\boldsymbol{x}}$ defined in Eq. (5).

in the FSS limit, we obtain

$$\chi \sim L^{\kappa_v}, \quad \kappa_v = 3 - 2Y_{V,XY} = 1.96182(2), \quad (19)$$

along the DD-O transition line, and

$$\chi \sim L^{\kappa_t}, \quad \kappa_t = 3 - 2Y_{T,XY} = 0.5274(2), \quad (20)$$

along the DO-O transition line. Also scaling corrections are expected to be different in the two cases. Along the DD-O transition line, corrections are expected to scale as $L^{-\omega_{XY}}$, where [95] $\omega_{XY} = 0.789(4)$ is associated with the leading irrelevant operator. On the other hand, along the DO-O line the dominant scaling corrections to Eq. (20) are due to the background analytic term [93]. Thus, corrections scale as $L^{-\kappa_t}$, with $\kappa_t \approx 0.527 < \omega_{XY} \approx 0.789$. As we have discussed in Sec. III C, along the DO-O line there are also emerging vector critical modes, that shows up only if a proper gauge fixing is introduced. They are discussed in Sec. VI.

IV. NUMERICAL RESULTS FOR THE $\mathbb{Z}_2$-GAUGE N=2 VECTOR MODEL

To investigate the nature of the transition lines of the $\mathbb{Z}_2$-gauge model for $N = 2$, we have performed MC simulations close to the transition lines DD-O and DO-O, on lattices of size $L \leq 40$. Simulations have been performed by using a standard Metropolis update for the gauge variables $\sigma_{\boldsymbol{x},\mu}$, and a combination of Metropolis and microcanonical updates (in the ratio 1:5) for the variables $\boldsymbol{s}_{\boldsymbol{x}}$. In all cases we performed MC runs of about 5×10^6 sweeps (a sweep corresponds to a complete update of all lattice gauge and spin variables). Simulations took a total CPU time of roughly 1.5×10^5 core-hours.

We have studied the critical behavior fixing K and varying J. In Table I, we report the values of K considered, the transition points $J_c(K)$, and some information on the critical behavior.

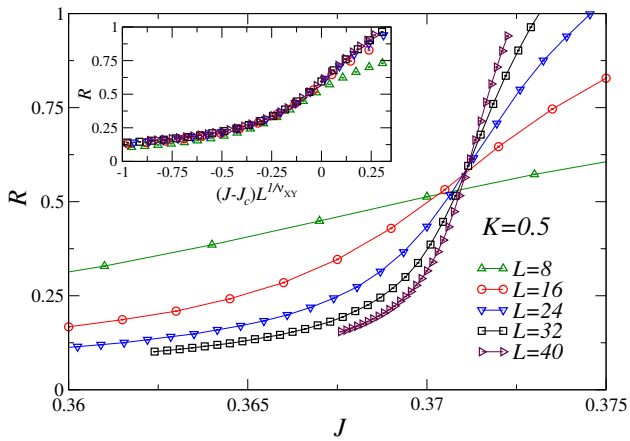

FIG. 3: Data of the ratio $R \equiv \xi/L$ as a function of J at fixed $K = 0.5$. The inset shows that the data nicely collapse onto a single curve when R is plotted $W = (J - J_c)L^{1/\nu_{XY}}$, with $J_c = 0.37118$ and $\nu_{XY} = 0.6717$, confirming the XY nature of the transition.

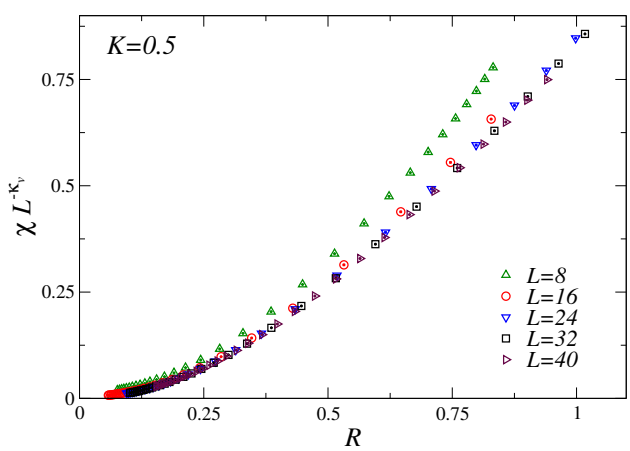

FIG. 4: Scaling of the susceptibility χ along the $K = 0.5$ line: plot of $L^{-\kappa_v}\chi$ versus $R = \xi/L$, with $\kappa_v = 3 - 2Y_{V,XY} = 1.96182$. Here $Y_{V,XY}$ is the RG dimension of the vector field in the XY universality class. The data approach an asymptotic scaling curve with increasing L, thus supporting relation (19).

A. The small-K DD-O transition line

We now report the results of the FSS analyses of the data obtained by varying J across the DD-O transition line, keeping K fixed. We considered three values of K, $K = 0$, $K = 0.5$, and $K = 0.7$, which are smaller than the value $K_\star \approx 0.75$ of the meeting point of the three transition lines, see Sec. III E and Sec. V. We anticipate that the FSS analyses show that the system undergoes continuous XY transitions for $K = 0$ and $K = 0.5$, and a first-order transition for $K = 0.7$. Thus, the continuous XY transition line starting at $K = 0$ turns into a first-order line at $K = K_{\rm fo}$ with $0.5 < K_{\rm fo} < 0.7$, before reaching the point where the transition lines meet, see Sec. V.

We first report results along the line $K = 0.5$. To determine the critical point and the order of the transition, we consider the RG invariant quantities R and U defined in Eqs. (8) and (9). At continuous transitions they are expected to scale as

$$R(J, L) = \mathcal{R}(W) + O(L^{-\omega}), \quad W = (J - J_c)L^{1/\nu}, \quad (21)$$
$$U(J, L) = \mathcal{U}(W) + O(L^{-\omega}). \quad (22)$$

In particular, the curves obtained for different lattice sizes should cross at the critical point, apart from scaling corrections. In Fig. 3 we plot R as a function of J. The data show a crossing point, indicating the presence of a continuous transition at $J_c \approx 0.37$. Analogous results are obtained for the Binder parameter. The slopes of the data at the crossing point are fully consistent with the length-scale exponent [95] $\nu_{XY} = 0.6717(1)$ of the XY universality class. To obtain a precise estimate of J_c, we have fitted the data to Eq. (22) setting $\nu = \nu_{XY} = 0.6717$. We obtain $J_c = 0.37118(2)$. A scaling plot is shown in the inset of Fig. 3. We observe a very nice collapse of the data, confirming that the transition belongs to the XY universality class.

The RG dimension Y_Q of the operator $Q^{ab}_{\boldsymbol{x}}$ can be estimated by fitting the susceptibility to Eq. (18). However, from a numerical point of view, it is more convenient to consider the FSS behavior of χ in terms of $R \equiv \xi/L$. Indeed, since R is monotonic, we can express W as a function of R using Eq. (21). Thus, we can rewrite Eq. (18) as

$$\chi(J, L) \approx L^{-(d-2Y_Q)} \left[\widehat{\mathcal{A}}(R) + O(L^{-\omega})\right]. \quad (23)$$

The data shown in Fig. 4 are consistent with Eq. (23) using the exponent reported in Eq. (19), i.e., $d - 2Y_Q = \kappa_v = 1.96182(2)$. Thus, the correlations of $Q^{ab}_{\boldsymbol{x}}$ behave as vector correlations in the standard XY model.

A robust check that the transition belongs to the XY universality class can be obtained by comparing the asymptotic behavior of U as a function of R in the present model with the analogous data computed in the XY model. We show the data in Fig. 5, together with the parameterization of the XY curve $U = f_{XY}(R)$ reported in Ref. [75]. The data for the $\mathbb{Z}_2$-gauge $N = 2$ vector model appear to approach the XY scaling curve as L increases. We observe some deviations, especially for $L = 8$ and $R \approx 0.25$, which apparently decrease as L increases. To verify that these deviations can be interpreted as scaling corrections, we consider the quantity

$$\Delta U(J, L) = L^{\omega_{XY}}[U(J, L) - f_{XY}(R(J, L))]. \quad (24)$$

In the inset of Fig. 5 we report ΔU as a function of R, using the expected XY correction-to-scaling exponent $\omega_{XY} \approx 0.789$. Data fall approximately onto a single curve as L increases, providing evidence that the deviations in Fig. 5 are due to scaling corrections. We remark that FSS curves depend on boundary conditions. Since we use here periodic boundary conditions, we compare

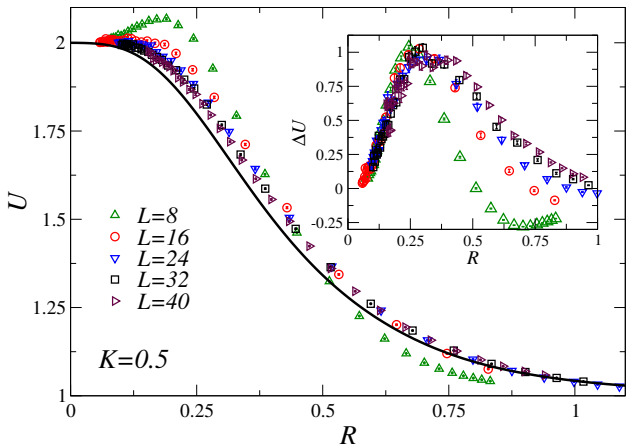

FIG. 5: The Binder parameter U as a function of $R = \xi/L$ for $K = 0.5$. The data appear to approach the universal scaling curve (solid line) for the XY model obtained in Ref. [75]. The observed deviations can be explained by the presence of scaling corrections: In the inset we report ΔU defined in Eq. (24) as a function of R, using the XY leading scaling-correction exponent $\omega_{XY} = 0.789$.

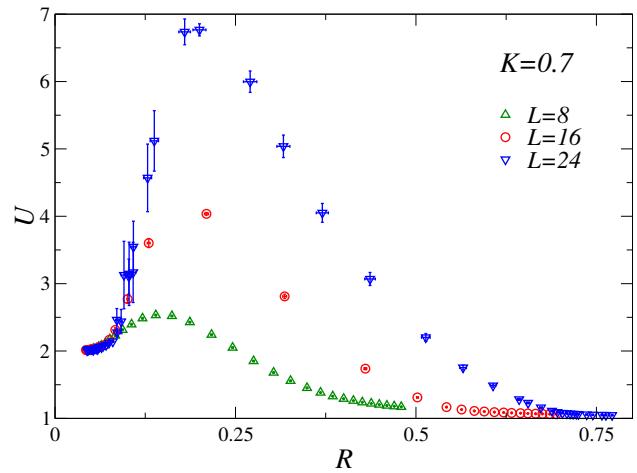

FIG. 6: The Binder parameter U versus R for $K = 0.7$. The data do not show scaling, and the maximum of U significantly increases with the size, as expected at a first-order transition.

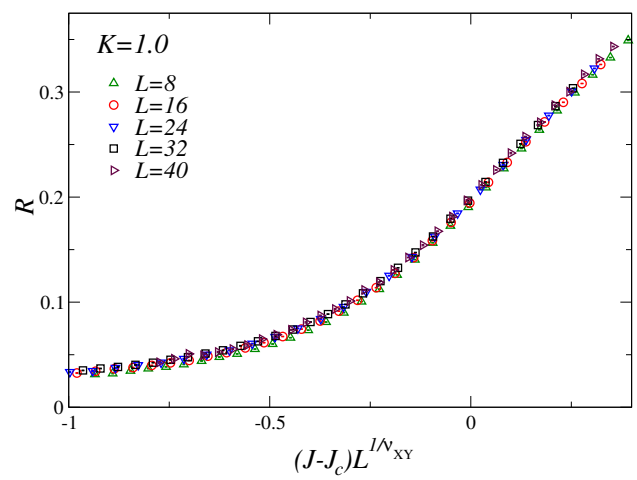

FIG. 7: Ratio $R \equiv \xi/L$ versus $W = (J-J_c)L^{1/\nu_{XY}}$, with $J_c = 0.22729(3)$ and $\nu_{XY} = 0.6717$. Results for $K = 1$. Data show an excellent collapse, confirming that the transition belongs to the XY universality class.

the data with XY results with the same boundary conditions (this is indeed the case for the curve obtained in Ref. [75]).

We also performed simulations along the $K = 0$ line, close to the critical transition at $J_c = 0.79305(7)$. The plots of R, U, and χ are very similar to those reported in Figs. 3, 4, and 5, so we do not report them. Again, they confirm the general analysis reported in Sec. III.

Finally, we performed simulations along the line $K = 0.7$. Data suggest a first-order transition with $J_c \approx 0.25$. The first-order nature of the transition can be inferred from the behavior of the Binder parameter U. As shown in Fig. 6, fixed-L data have a pronounced maximum, which significantly increases with increasing L. This is usually considered as evidence of a first-order transition, see, for example, Ref. [109] and references therein. To estimate J_c, we have determined the position $J_p(L)$ of the maximum of U for each size, and then we have extrapolated the results to $J_p(L) = J_c + a/L^3$. We obtain the estimate $J_c = 0.2520(3)$.

B. The large-K DO-O transition line

We now discuss the critical behavior along the DO-O transition line. We have performed simulations varying J along the lines $K = 1$ and $K = 0.8$. These values of K are larger than the value $K_\star \approx 0.75$ corresponding to the meeting point of the three transition lines, see Sec. III E and Sec. V. Therefore, for both values of K, we are considering DO-O transitions. In both cases, the FSS analyses show a continuous XY transition where the operator $Q^{ab}_{\boldsymbol{x}}$ behaves as a spin-two operator, in agreement with the arguments reported in Sec. III F.

For $K = 1$, data are consistent with a continuous transition in the XY universality class. We can accurately estimate the critical point from the analysis of $R = \xi/L$. Fits of R to Eq. (21) using the XY exponent $\nu_{XY} = 0.6717$ give $J_c = 0.22729(3)$. The corresponding scaling plot is shown in Fig. 7. Scaling is excellent. We note that $J_c(K = 1)$ is very close to the critical value for $K = \infty$, i.e., [95] $J_c(K = \infty) = 0.22708234(9)$. This indicates that the DO-O line $J = J_c(K)$ has a very weak dependence on K from $K = \infty$ to $K = 1$ (as supposed in Sec. III E).

In Fig. 8 we report the Binder cumulant U against the ratio R. We observe a nice scaling that confirms the continuous nature of the transition. Note that in this case we cannot directly compare the results for $K = 1$ with the corresponding scaling curve computed in the XY model

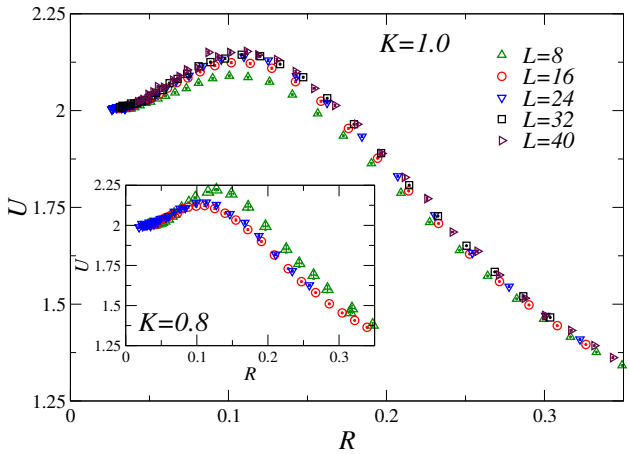

FIG. 8: The Binder cumulant U as a function of $R = \xi/L$ for $K = 1$. The data appear to collapse onto an asymptotic curve. The inset shows analogous data for $K = 0.8$, which appear to approach the same asymptotic FSS curve.

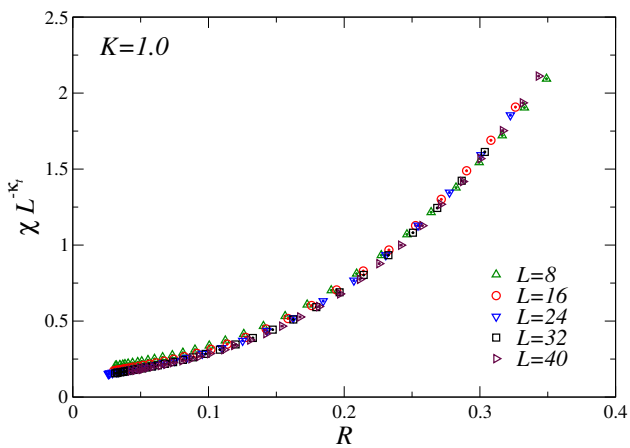

FIG. 9: Scaling of the susceptibility χ. We plot $L^{-\kappa_t}\chi$ versus $R = \xi/L$, with $\kappa_t = 3 - Y_{T,XY} = 0.5274$. The excellent collapse of the data confirms the correctness of the predicted exponent κ_t, see Eq. (20).

with periodic boundary conditions. Indeed, for $K \to \infty$ the $\mathbb{Z}_2$-gauge model with periodic boundary conditions is equivalent to an N-vector model with fluctuating boundary conditions, see the discussion in Ref. [75]. Therefore, to perform a correct comparison one should simulate an XY model with fluctuating boundary conditions, to determine the XY curve that matches the $\mathbb{Z}_2$-gauge data.

In Fig. 9 we show a scaling plot of the susceptibility defined in Eq. (7). As discussed in Sec. III F, data should scale according to Eq. (23), with exponent $d-2Y_Q = \kappa_t = d-2Y_{T,XY} = 0.5274(2)$. We observe an excellent scaling, confirming the arguments of Sec. III F.

Finally, we performed simulations along the line $K = 0.8$ on relatively small lattices. Data indicate the presence of a continuous XY transition at $J_c \approx 0.229$ (the relatively low precision on J_c is due to the small lattices considered), analogous to the one observed for $K = 1$.. This is clearly demonstrated by the plots of U versus R shown in the inset of Fig. 8. The $K = 0.8$ data approach the same asymptotic curve obtained for $K = 1$.

V. TRANSITIONS AT THE MEETING POINT

We now discuss the nature of the transitions close to the point $(K_\star, J_\star)$, where the transition lines meet, see Fig. 1. On the basis of the arguments reported in Sec. III, the DD-O transitions are of first order for any $N \geq 3$, while they may be continuous for $N = 2$. On the other hand, for any N we expect DO-O and DD-DO transitions to be continuous for large K and small J, respectively. Close to the meeting point, they may be continuous or of first order, with the corresponding presence of a tricritical point.

We wish now to estimate the position of the meeting point $(K_\star, J_\star)$. The results reported in Table I show that the point $[K = 0.5, J = 0.37118(2)]$ belongs to the DD-O line, while the point $[K = 0.8, J \approx 0.229]$ belongs to the DO-O line. This allows us to bound $J_\star$: $0.371 > J_\star > 0.229$. We can then use the approximate formula (10) to obtain a bound on $K_\star$: $0.724 < K_\star < 0.756$. This estimate of $K_\star$ allows us to conclude that the first-order transition observed at $(K = 0,7, J = 0.2520(3))$ belongs to the DD-O line. Therefore, there is a tricritical point at $K = K_{fo}$, $0.5 < K_{fo} < 0.7$ on the DD-O line, such that DD-O transitions are continuous for $K < K_{fo}$ and of first order in the opposite case. The results for $K = 0.7$ allow us to improve our estimate of $J_\star$, which should belong to the interval $[J_c(0.8), J_c(0.7)] = [0.229, 0.252]$. In turn, we can use this result to improve our estimate of $K_\star$. We obtain finally the estimates

$$(K_\star \approx 0.75,\ J_\star \approx 0.24) \quad \text{for} \quad N = 2. \tag{25}$$

To verify the accuracy of these arguments, we have applied similar arguments to the $\mathbb{Z}_2$ gauge Higgs model. For the multicritical point, we obtain $K_\star \approx 0.75$, in good agreement with the accurate estimate $K_\star = 0.7525(1)$, see Fig. 2.

Given that the DD-O transition line is of first order, the nature of the meeting-point transition is controlled by the competition of the N-vector order parameter driving the DO-O transitions (the emerging order parameter discussed in Sec. III C) and the nonlocal order parameter driving the Ising topological transitions along the DD-DO transition line. We are not able to define an effective model appropriate to describe the meeting-point transition. In general, two different behaviors are possible. In one case, the DD-DO and DO-O line are continuous up to the meeting point, so that we obtain what is usually called a bicritical point. Alternatively, the continuous transitions may turn into first-order ones before the meeting point, as it occurs along the DD-O transition lines, see Fig. 10. In this case, one would observe a discontinuous behavior at the meeting point. Our numerical data do not allow us to distinguish between the

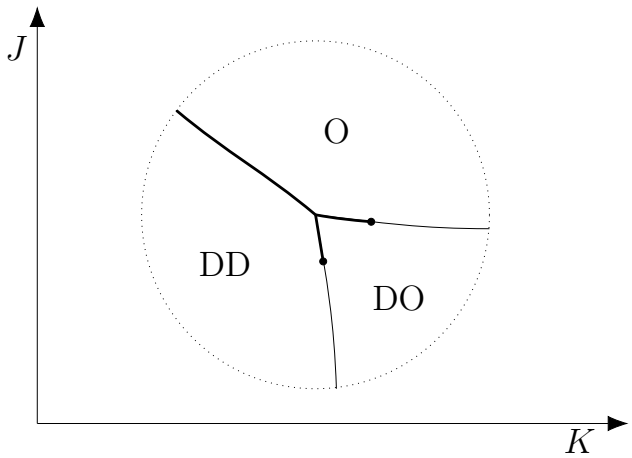

FIG. 10: Sketch of the phase diagram close to a first-order meeting point.

two scenarios. We only observe that, if the DO-O line becomes eventually of first order by decreasing K, this should occur very close to the meeting point.

It is interesting to observe that a first-order meeting point is expected when the transitions are associated with one N vector parameter ϕ_1 and one scalar order parameter ϕ_2, which are both local. Indeed, the corresponding LGW model [110–112], with Hamiltonian

$$L = \frac{1}{2}\sum_\mu [(\partial_\mu \phi_1)^2 + (\partial_\mu \phi_2)^2] + \frac{1}{2}(r_1\phi_1^2 + r_2\phi_2^2) + u_1(\phi_1^2)^2 + u_2\phi_2^4 + w\phi_1^2\phi_2^2, \tag{26}$$

does not admit any fixed point for any $N \geq 2$, see, e.g., Refs. [93, 107, 113, 114]. Only the multicritical $Z_2 \oplus Z_2$ LGW theory, corresponding to $N = 1$, has a stable bicritical fixed point belonging to the XY universality class. This effective LGW model has been used to investigate the nature of the transitions close to the meeting point in the Z_2 gauge Higgs model. In that case, however, duality allowed us to argue that the nonlocal order parameter could be mapped by duality onto a local one. Duality is missing here and therefore the relation between the local LGW model and our gauge model is unclear.

VI. VECTOR CORRELATIONS IN THE PRESENCE OF A STOCHASTIC GAUGE FIXING

In this section we would like to come back to the question of the appropriate order parameter for the DO-O transitions. As discussed in Sec. III C, a correct LGW description requires a vector order parameter, but this is apparently at odds with the gauge invariance of the model. Indeed, the lattice vector field $\boldsymbol{s}_x$ is not gauge invariant and therefore its correlation functions are trivial. In particular, its two-point function

$$G_s(\boldsymbol{x}, \boldsymbol{y}) = \langle \boldsymbol{s}_{\boldsymbol{x}} \cdot \boldsymbol{s}_{\boldsymbol{y}} \rangle \tag{27}$$

trivially vanishes for $\boldsymbol{x} \neq \boldsymbol{y}$. This apparent puzzle can be solved by showing that critical vector correlations can be uncovered by an appropriate gauge fixing. For this purpose, we implement the stochastic gauge fixing outlined in Ref. [87]. It leaves gauge-invariant correlations invariant, it is thermodynamically well defined, and allows us to unveil the critical vector modes that effectively drive the DO-O transitions.

Because of the discrete nature of the gauge variables, standard gauge fixing procedures cannot be applied. Therefore the idea is to average non-gauge invariant quantities over all possible gauge transformations, i.e.

$$\begin{aligned} \boldsymbol{s}_{\boldsymbol{x}} &\to \hat{\boldsymbol{s}}_{\boldsymbol{x}} = w_{\boldsymbol{x}} \boldsymbol{s}_{\boldsymbol{x}}, \\ \sigma_{\boldsymbol{x},\mu} &\to \hat{\sigma}_{\boldsymbol{x},\mu} = w_{\boldsymbol{x}} \sigma_{\boldsymbol{x},\mu} w_{\boldsymbol{x}+\hat{\mu}}, \end{aligned} \tag{28}$$

using an appropriate weight for the $\mathbb{Z}_2$ site variables $w_{\boldsymbol{x}} = \pm 1$. As discussed in Ref. [87], a convenient choice is provided by the Gibbs weight $\exp[-H_w(\sigma, w)]$, with the ancillary Hamiltonian

$$H_w = -\gamma \sum_{\boldsymbol{x},\mu} w_{\boldsymbol{x}} \sigma_{\boldsymbol{x},\mu} w_{\boldsymbol{x},\mu}, \qquad \gamma > 0, \tag{29}$$

so that positive values of $\hat{\sigma}_{\boldsymbol{x},\mu} = w_{\boldsymbol{x}} \sigma_{\boldsymbol{x},\mu} w_{\boldsymbol{x}+\hat{\mu}}$ are favored. Correspondingly, we define a gauge-fixed two-point spin function $\widehat{G}_s$ as

$$\widehat{G}_s(\boldsymbol{x}, \boldsymbol{y}) = \langle [\hat{\boldsymbol{s}}_{\boldsymbol{x}} \cdot \hat{\boldsymbol{s}}_{\boldsymbol{y}}] \rangle = \frac{\sum_{\{\boldsymbol{s},\sigma\}} e^{-H(\boldsymbol{s},\sigma)} [\hat{\boldsymbol{s}}_{\boldsymbol{x}} \cdot \hat{\boldsymbol{s}}_{\boldsymbol{y}}]}{\sum_{\{\boldsymbol{s},\sigma\}} e^{-H(\boldsymbol{s},\sigma)}} \tag{30}$$

where $\hat{\boldsymbol{s}}_{\boldsymbol{x}} = w_{\boldsymbol{x}} \boldsymbol{s}_{\boldsymbol{x}}$, H is the gauge-invariant Hamiltonian (2), and

$$[\hat{\boldsymbol{s}}_{\boldsymbol{x}} \cdot \hat{\boldsymbol{s}}_{\boldsymbol{y}}] = \frac{\sum_{\{w\}} e^{-H_w(\sigma,w)} \hat{\boldsymbol{s}}_{\boldsymbol{x}} \cdot \hat{\boldsymbol{s}}_{\boldsymbol{y}}}{\sum_{\{w\}} e^{-H_w(\sigma,w)}}. \tag{31}$$

Here $[\cdot]$ indicates the (quenched) average over the $\mathbb{Z}_2$ fields with weight e^{-H_w}, for fixed values of $\boldsymbol{s}_{\boldsymbol{x}}$ and $\sigma_{\boldsymbol{x},\mu}$, while $\langle \cdot \rangle$ is the standard average over $\boldsymbol{s}_{\boldsymbol{x}}$ and $\sigma_{\boldsymbol{x},\mu}$ with the gauge-invariant weight e^{-H}.

Note that the resulting model with the added variables $w_{\boldsymbol{x}}$ is a quenched random-bond Ising model [115] ($w_{\boldsymbol{x}}$ are the Ising variables), with a particular choice of bond distribution, determined by the gauge-invariant average over the variables $\boldsymbol{s}_{\boldsymbol{x}}$ and $\sigma_{\boldsymbol{x},\mu}$ of the $\mathbb{Z}_2$-gauge N-vector model. We recall that quenched random-bond Ising models have several phases—disordered, ferromagnetic, and glassy phases—depending on the temperature, the amount of randomness of the bond distribution, and its spatial correlations, see, e.g., Refs. [116–118]. In particular, we expect the present model to undergo a quenched transition for $\gamma = \gamma_c(J, K)$. The transition separates a disordered phase for $\gamma < \gamma_c(J, K)$ from a large-γ phase, which, a priori, can be ferromagnetic or glassy, depending on the nature of the bond coupling.

A key point of the above procedure concerns the value of γ, which should be chosen such that the spins $\boldsymbol{s}_{\boldsymbol{x}}$ become critical at the transition. For this purpose, γ must

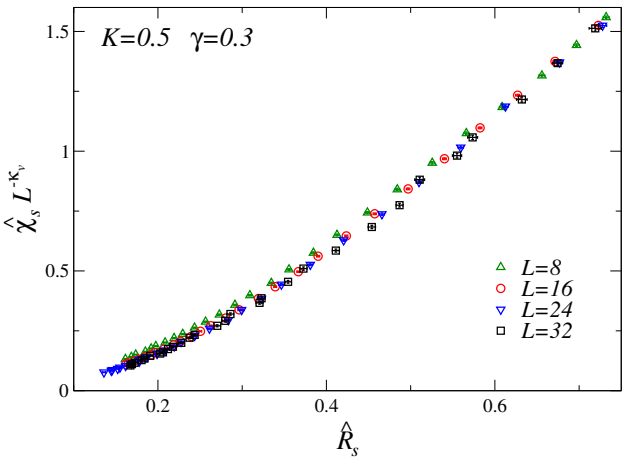

FIG. 11: Plot of $L^{-\kappa_v}\chi_s$ versus $\hat{R}_s = \hat{\xi}_s/L$ for $K = 1$, $\gamma = 0.3$. Here $\hat{\chi}_s$ and $\hat{\xi}_s$ are defined in terms of $\widehat{G}_s$, see Eq. (30). We set $\kappa_v = 3 - 2Y_{V,XY} = 1.96182(2)$, where $Y_{V,XY}$ is the RG dimension of the vector field in the XY universality class.

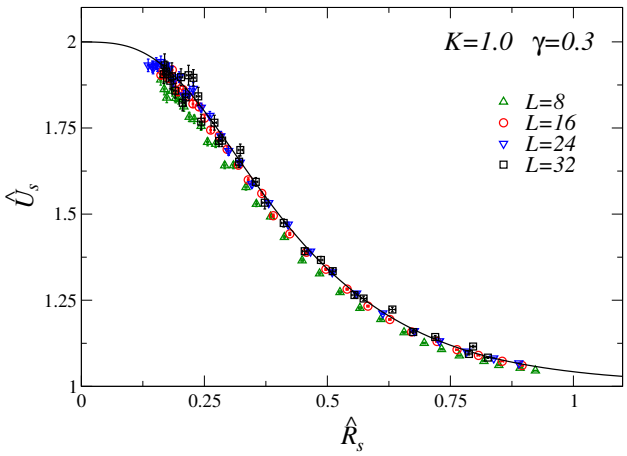

FIG. 12: The Binder parameter $\hat{U}_s$ as a function of $\hat{R}_s \equiv \hat{\xi}_s/L$ for $K = 1$ and $\gamma = 0.3$. The data appear to approach the universal scaling curve (solid line) for the XY model obtained in Ref. [75].

be large—more precisely, it should satisfy $\gamma > \gamma_c(J, K)$—to ensure that the variables $w_{\boldsymbol{x}}$ are ordered, effectively favouring positive values for the link variables $\hat{\sigma}_{\boldsymbol{x},\mu} = w_{\boldsymbol{x}}\sigma_{\boldsymbol{x},\mu}w_{\boldsymbol{x}+\hat{\mu}}$. On the other hand, for $\gamma < \gamma_c(J, K)$, we do not expect vector correlations to become critical.

Quenched averages are computed as in standard simulations of random quenched systems. We simulate the model with Hamiltonian H and every N_s sweeps we compute the gauge averages over the $w_{\boldsymbol{x}}$ variables for fixed values of $\boldsymbol{s}_{\boldsymbol{x}}$ and $\sigma_{\boldsymbol{x},\mu}$ (at fixed disorder in the language of random systems). We use a standard Metropolis update. For each "disorder realization," we perform about 10^5 sweeps of the whole lattice. After discarding approximately $O(10^4)$ sweeps to ensure thermalization, we perform approximately 10^2 measurements (this is probably much more than needed, but it guarantees the absence of any initialization bias).

In the following we show that, for sufficiently large values of γ, along the DO-O transition line the two-point function $\widehat{G}_s$ behaves as the vector correlation function in the XY model. For this purpose, it is useful to define the susceptibility $\hat{\chi}_s$ and the second-moment correlation length $\hat{\xi}_s$, which can be defined as in Eq. (7) in terms of $\widehat{G}_s$. We also define the Binder parameter associated with the spin variables $\hat{\boldsymbol{s}}_{\boldsymbol{x}}$

$$\hat{U}_s = \frac{\langle [m_{2s}^2] \rangle}{\langle [m_{2s}] \rangle^2}, \qquad m_{2s} = \frac{1}{L^d} \sum_{\boldsymbol{x},\boldsymbol{y}} \hat{\boldsymbol{s}}_{\boldsymbol{x}} \cdot \hat{\boldsymbol{s}}_{\boldsymbol{y}}. \tag{32}$$

We show now results at the transition for $K = 1$. We first verified that the model with $K = 1$ and $J = J_c$ has a transition for $\gamma = \gamma_c \approx 0.22$, which separates a disordered small-γ phase from a ferromagnetically ordered large-γ phase. We thus fixed $\gamma = 0.3$. To verify that such value corresponds to a ferromagnetic ordered phase, we have considered the Binder parameter for the overlap of the variables $w_{\boldsymbol{x}}$, which appears to approach the value $U_w = 1$ as $L \to \infty$, with inverse-volume corrections, as expected for a ferromagnetic phase.

In Fig. 11 we show the results for the susceptibility $\hat{\chi}_s$ for $K = 1$ and $\gamma = 0.3$. They demonstrate that it behaves as the XY vector susceptibiliy. Indeed, we find that $\hat{\chi}_s \sim L^{\kappa_v}$ with $\kappa_c = 3 - 2Y_{V,XY} = 2 - \eta_{XY}$. This is also confirmed by the plot of $\hat{U}_s$ versus $R_s \equiv \xi_s/L$ reported in Fig. 12. Indeed, the data converge toward the corresponding XY universal curve. These results are expected to hold for any value of γ, as long as $\gamma > \gamma_c \approx 0.22$ for $K = 1$.

Along the small-K DD-O line the data suggest a discontinuous behavior of $\widehat{G}_s$ for $\gamma \gtrsim 0.3$. This result is consistent with the general picture. Indeed, the results along the DO-O line indicate that vector modes magnetize as J increases across the DO-O line. Physically, we do not expect the gauge-fixing procedure to give rise to additional transition lines in the O phase. Therefore, vector modes should also magnetize as J increases across the DD-O line. However, along the DD-O line, the operator $Q_{\boldsymbol{x}}^{ab}$ is the order parameter which behaves as a vector XY field, so there cannot be an additional emerging critical vector field. Thus, $\widehat{G}_s$ is discontinuous, but not critical.

We finally remark that analogous results are expected at the O(N) continuous transitions along the DO-O transition line for higher values of N. See in particular Ref. [87] for other applications of the stochastic gauge fixing.

VII. CONCLUSIONS

We have investigated the phase diagram and critical behavior of 3D lattice $\mathbb{Z}_2$-gauge N-vector models. Their Hamiltonian Eq. (2) is obtained by minimally coupling N-component real variables with $\mathbb{Z}_2$ gauge variables,

with a global O(N) and local $\mathbb{Z}_2$ invariance. They represent paradigmatic models with different phases characterized by the spontaneous breaking of the global O(N) symmetry and by the different topological properties of the $\mathbb{Z}_2$-gauge excitations.

The 3D $\mathbb{Z}_2$-gauge N-vector model presents three phases for any $N \geq 2$, distinguished by the order/disorder of the spin correlations and the order/disorder of the $\mathbb{Z}_2$-gauge correlations, see Fig. 1. These phases are separated by three transition lines.

(i) At small J, the small-K and large-K spin-disordered phases are separated by a line of topological transitions. Their continuous transitions belong to the $\mathbb{Z}_2$-gauge universality class for any N.

(ii) The transitions along the small-K DD-O line are first order for any $N \geq 3$. For $N = 2$ we observe continuous transitions for sufficiently small K, belonging to the 3D XY universality class; they turn into first-order ones as K is increased, before reaching the meeting point.

(iii) The transitions along the large-K DO-O line are expected to be continuous for any N (at least for sufficiently large K). These transitions belong to the O(N) vector universality class. It is important to note that these O(N) transitions are quite peculiar, since critical vector correlations emerge only after an appropriate gauge fixing and, in particular, when the stochastic gauge fixing outlined in the companion paper [87] is used. This gauge fixing approach is thermodynamically consistent and local, thus it allows us to apply standard RG arguments to the stochastically gauge-fixed theory.

In this work we mainly focus on models with $N = 2$. At variance with what happens when $N \geq 3$, in this case the small-K DD-O transitions can be continuous—for larger values of N they are of first order. Interestingly, the small-K DD-O transitions and the large-K DO-O transitions both belong to the XY universality class. In spite of this, the critical behavior along the two lines is different. Indeed, for small values of K the vector XY order parameter is gauge invariant. Instead, for large values of K, the model has an emergent order parameter, the spin $\boldsymbol{s}_{\boldsymbol{x}}$ within an appropriate stochastic gauge fixing because it is not gauge-invariant. The different nature of the critical modes can be probed by studying the correlations of the gauge-invariant operator $Q^{ab}_{\boldsymbol{x}}$. Along the small-K DD-O transition line, its RG dimension Y_Q coincides with the RG dimension $Y_{V,XY} = 0.519088(22)$ of the vector field in the XY universality class. On the other hand, along the large-K DO-O line, since the order parameter is the spin $s_{\boldsymbol{x}}$, $Q^{ab}_{\boldsymbol{x}}$ behaves as a tensor spin-2 operator. Therefore, we predict $Y_Q = Y_{T,XY}$ where $Y_{T,XY} = 1.23629(11)$, where $Y_{T,XY}$ is the spin-two RG dimension in the XY universality class. This different behavior is easily detected by studying the size dependence of the corresponding susceptibility, which diverges as $\chi \sim L^{1.9618}$ along the small-K DD-O transition line and as $\chi \sim L^{0.5274}$ along the large-K DO-O transition line.

To verify the previous predictions we have performed MC simulations for $N = 2$, see Table I. The FSS analyses of the data confirm the general results presented above and, in particular, the two different effective XY descriptions of the small-K DD-O and large-K DO-O transition lines.

Acknowledgments

The authors acknowledge support from project PRIN 2022 "Emerging gauge theories: critical properties and quantum dynamics" (20227JZKWP). Numerical simulations have been performed on the CSN4 cluster of the Scientific Computing Center at INFN-PISA.

[1] S. Weinberg, *The Quantum Theory of Fields*, (Cambridge University Press, 2005)
[2] P. W. Anderson, *Basic Notions of Condensed Matter Physics*, (The Benjamin/Cummings Publishing Company, Menlo Park, California, 1984)
[3] X.-G. Wen, *Quantum field theory of many-body systems: from the origin of sound to an origin of light and electrons*, (Oxford University Press, 2004)
[4] E. Fradkin, *Field theories of condensed matter physics* (Cambridge University Press, 2013).
[5] S. Sachdev, Topological order, emergent gauge fields, and Fermi surface reconstruction, Rep. Prog. Phys. **82**, 014001 (2019).
[6] F. J. Wegner, Duality in generalized ising models and phase transitions without local order parameters, Jour. of Math. Phys. **12**, 2259 (1971).
[7] B. I. Halperin, T. C. Lubensky, and S. K. Ma, First-Order Phase Transitions in Superconductors and Smectic-A Liquid Crystals, Phys. Rev. Lett. **32**, 292 (1974).
[8] R. Balian, J. M. Drouffe, and C. Itzykson, Gauge fields on a lattice. i. general outlook, Phys. Rev. D **10**, 3376 (1974); Gauge fields on a lattice. II. Gauge-invariant Ising model, Phys. Rev. D **11**, 2098 (1975).
[9] E. Fradkin and S. Shenker, Phase diagrams of lattice gauge theories with Higgs fields, Phys. Rev. D **19**, 3682 (1979).
[10] J. B. Kogut, An introduction to lattice gauge theory and spin systems, Rev. Mod. Phys. **51**, 659 (1979).
[11] C. Dasgupta and B. I. Halperin, Phase Transitions in a Lattice Model of Superconductivity, Phys. Rev. Lett **47**, 1556 (1981).
[12] J. Bricmont and J. Fröhlich, An order parameter distinguishing between different phases of lattice gauge theories with matter fields, Phys. Lett. **122**, 73 (1983)
[13] K. Fredenhagen and M. Marcu, Charged states in Z_2 gauge theories, Commun. Math. Phys. **92**, 81 (1983).
[14] C. Borgs and F. Nill, The Phase Diagram of the Abelian

Lattice Higgs Model. A Review of Rigorous Results, J. Stat. Phys. 47, 877 (1987)
[15] N. Read and S. Sachdev, Spin-Peierls, valence-bond solid, and Néel ground states of low-dimensional quantum antiferromagnets, Phys. Rev. B **42**, 4568 (1990).
[16] G. Murthy and S. Sachdev, Actions of hedgehogs instantons in the disordered phase of 2+1 dimensional CP^{N-1} model, Nucl. Phys. B **344**, 557 (1990).
[17] D. A. Huse and St. Leibler, Are sponge phases of membranes experimental gauge-higgs systems?, Phys. Rev. Lett. **66**, 437 (1991).
[18] X.-G. Wen, Mean-field theory of spin-liquid states with finite energy gap and topological orders, Phys. Rev. B **44**, 2664 (1991).
[19] P. E. Lammert, D. D. Roskar, and J. Toner, Topology and nematic ordering, Phys. Rev. Lett. **70**, 1650 (1993); Topology and nematic ordering. I. A gauge theiry, Phys. Rev. E **52**, 1778 (1995); Topology and nematic ordering. II. Observable critical behavior, Phys. Rev. E **52**, 1801 (1995).
[20] B. Bergerhoff, F. Freire, D.F. Litim, S. Lola, and C. Wetterich, Phase diagram of superconductors from nonperturbative flow equations, Phys. Rev. B **53**, 5734 (1996).
[21] F. Herbut and Z. Tesanovic, Critical Fluctuations in Superconductors and the Magnetic Field Penetration Depth, Phys. Rev. Lett. **76**, 4588 (1996).
[22] T. Senthil and M. P. A. Fisher, Z_2 gauge theory of electron fractionalization in strongly correlated systems, Phys. Rev. B **62**, 7850 (2000).
[23] J. Hove and A. Sudbo, Anomalous Scaling Dimensions and Stable Charged Fixed Point of Type-II Superconductors, Phys. Rev. Lett. **84**, 3426 (2000).
[24] R. Moessner, S. L. Sondhi, and E. Fradkin, Short-ranged resonating valence bond physics, quantum dimer models, and ising gauge theories, Phys. Rev. B **65**, 024504 (2001).
[25] R. D. Sedgewick, D. J. Scalapino, and R. L. Sugar, Fractionalized phase in an $XY-Z_2$ gauge model, Phys. Rev. B **65**, 054508 (2002).
[26] T. Senthil and O. Motrunich, Microscopic models for fractionalized phases in strongly correlated systems, Phys. Rev. B **66**, 205104 (2002).
[27] H. Kleinert, F. S. Nogueira, and A. Sudbø, Deconfinement Transition in Three-Dimensional Compact U(1) Gauge Theories Coupled to Matter Fields, Phys. Rev. Lett. **88**, 232001 (2002).
[28] S. Mo, J. Hove, and A. Sudbø, Order of the metal-to-superconductor transition, Phys. Rev. B **65**, 104501 (2002).
[29] A. Sudbø, E. Smørgrav, J. Smiseth, F. S. Nogueira, and J. Hove, Criticality in the (2+1)-Dimensional Compact Higgs Model and Fractionalized Insulators, Phys. Rev. Lett. **89**, 226403 (2002).
[30] A. Kitaev, Fault-tolerant quantum computation by anyons, Ann. Phys. New York **303**, 2 (2003).
[31] J. Smiseth, E. Smørgrav, F. S. Nogueira, J. Hove, and A. Sudbø, Phase Structure of $d = 2+1$ Compact Lattice Gauge Theories and the Transition from Mott Insulator to Fractionalized Insulator, Phys. Rev. B **67**, 205104 (2003).
[32] T. Neuhaus, A. Rajantie, and K. Rummukainen, Numerical study of duality and universality in a frozen superconductor, Phys. Rev. B **67**, 014525 (2003).
[33] T. Senthil, L. Balents, S. Sachdev, A. Vishwanath, and M. P. A. Fisher, Quantum Criticality beyond the Landau-Ginzburg-Wilson Paradigm, Phys. Rev. B **70**, 144407 (2004).
[34] O. I. Motrunich and A. Vishwanath, Emergent photons and transitions in the O(3) σ-model with hedgehog suppression, Phys. Rev. B **70**, 075104 (2004).
[35] J. Smiseth, E. Smorgrav, and A. Sudbø, Critical properties of the N-color London model, Phys. Rev. Lett. **93**, 077002 (2004).
[36] Z. Nussinov, Derivation of the Fradkin-Shenker result from duality: Links to spin systems in external magnetic fields and percolation crossovers, Phys. Rev. D **72**, 054509 (2005).
[37] S. Takashima, I. Ichinose, and T. Matsui, CP^1+U(1) lattice gauge theory in three dimensions: Phase structure, spins, gauge bosons, and instantons, Phys. Rev. B **72**, 075112 (2005).
[38] S. Wenzel, E. Bittner, W. Janke, A. M. J. Schakel, and A. Schiller, Kertesz Line in the Three-Dimensional Compact U(1) Lattice Higgs Model, Phys. Rev. Lett. **95**, 051601 (2005).
[39] M. N. Chernodub, E.-M. Ilgenfritz, A. Schiller, Phase structure of an Abelian two-Higgs model and high temperature superconductors, Phys. Rev. B **73**, 100506 (2006).
[40] A. W. Sandvik, Evidence for Deconfined Quantum Criticality in a Two-Dimensional Heisenberg Model with Four-Spin Interactions, Phys. Rev. Lett. **98**, 227202 (2007).
[41] D. Charrier, F. Alet, and P. Pujol, Gauge Theory Picture of an Ordering Transition in a Dimer Model, Phys. Rev. Lett. **101**, 167205 (2008)
[42] R. K. Kaul and S. Sachdev, Quantum criticality of U(1) gauge theories with fermionic and bosonic matter in two spatial dimensions, Phys. Rev. B **77**, 155105 (2008).
[43] J. Vidal, S. Dusuel, and K. P. Schmidt, Low-energy effective theory of the toric code model in a parallel magnetic field, Phys. Rev. B **79**, 033109 (2009).
[44] T. Ono, S. Doi, Y. Hori, I. Ichinose, and T. Matsui, Phase Structure and Critical Behavior of Multi-Higgs U(1) Lattice Gauge Theory in Three Dimensions, Ann. Phys. (N.Y.) **324**, 2453 (2009).
[45] T. Grover and T. Senthil, Quantum phase transition from an antiferromagnet to a spin liquid in a metal, Phys. Rev. B **81**, 205102 (2010).
[46] I. S. Tupitsyn, A. Kitaev, N. V. Prokofev, and P. C. E. Stamp, Topological multicritical point in the phase diagram of the toric code model and three-dimensional lattice gauge Higgs model, Phys. Rev. B **82**, 085114 (2010).
[47] K. Gregor, D. A. Huse, R. Moessner, and S. L. Sondhi, Diagnosing deconfinement and topological order, New Jour. of Phys. **13**, 025009 (2011)
[48] S. Dusuel, M. Kamfor, R. Orus, K. P. Schmidt, and J. Vidal, Robustness of a perturbed topological phase, Phys. Rev. Lett. **106**, 107203 (2011).
[49] S. V. Isakov, R. G. Melko, and M. B. Hastings, Universal signatures of fractionalized quantum critical points, Science **335**, 193 (2012).
[50] S. Pujari, K. Damle, and F. Alet, Nèel-State to Valence-Bond-Solid Transition on the Honeycomb Lattice: Evidence for Deconfined Criticality, Phys. Rev. Lett. **111**, 087203 (2013).

[51] M. S. Block, R. G. Melko, and R. K. Kaul, Fate of CP^{N-1} fixed point with q monopoles, Phys. Rev. Lett. **111**, 137202 (2013).

[52] E. V. Herland, T. A. Bojesen, E. Babaev, and A. Sudbø, Phase structure and phase transitions in a three-dimensional SU(2) superconductor, Phys. Rev. B **87**, 134503 (2013).

[53] T. A. Bojesen and A. Sudbø, Berry phases, current lattices, and suppression of phase transitions in a lattice gauge theory of quantum antiferromagnets, Phys. Rev. B **88**, 094412 (2013).

[54] A. Nahum, J. T. Chalker, P. Serna, M. Ortuňo, and A. M. Somoza, Deconfined Quantum Criticality, Scaling Violations, and Classical Loop Models, Phys. Rev. X **5**, 041048 (2015).

[55] G. J. Sreejith and S. Powell, Scaling dimensions of higher-charge monopoles at deconfined critical points, Phys. Rev. B **92**, 184413 (2015).

[56] K. Liu, J. Nissinen, Z. Nussinov, R.-J. Slager, K. Wu, and J. Zaanen, Classification of nematic order in 2+1 dimensions: Dislocations melting and $O(2)/Z_N$ lattice gauge theory, Phys, Rev. B **91**, 075103 (2015).

[57] M. Schuler, S. Whitsitt, L.-P. Henry, S. Sachdev, and A. M. Läuchli, Universal signatures of quantum critical points from finite-size torus spectra: a window into the operator content of higher-dimensional conformal field theories, Phys. Rev. Lett. **117**, 210401 (2016).

[58] S. Whitsitt and S. Sachdev, Transition from the Z_2 spin liquid to antiferromagnetic order: spectrum on the torus, Phys. Rev. B **94** 085134 (2016).

[59] S. Sachdev, Emergent gauge fields and the high-temperature superconductors, Philosophical Transactions of the Royal Society A: Mathematical, Physical and Engineering Sciences **374**, 20150248 (2016)

[60] C. Wang, A. Nahum, M. A. Metliski, C. Xu, and T. Senthil, Deconfined Quantum Critical Points: Symmetries and Dualities, Phys. Rev. X **7**, 031051 (2017).

[61] G. Fejos and T. Hatsuda, Renormalization group flows of the N-component Abelian Higgs model, Phys. Rev. D **96**, 056018 (2017).

[62] A. Pelissetto, A. Tripodo, and E. Vicari, Landau-Ginzburg-Wilson approach to critical phenomena in the presence of gauge symmetries, Phys. Rev. D **96**, 034505 (2017).

[63] A. Pelissetto, A. Tripodo, and E. Vicari, Criticality of O(N) symmetric models in the presence of discrete gauge symmetries, Phys. Rev. E **97**, 012123 (2018).

[64] S. Gazit, F. F. Assaad, S. Sachdev, A. Vishwanath, C. Wang, Confinement transition of $\mathbb{Z}_2$ gauge theories coupled to massless fermions: emergent QCD_3 and $SO(5)$ symmetry Proc. Natl. Acad. Sci. **115**, E6987 (2018)

[65] B. Ihrig, N. Zerf, P. Marquard, I. F. Herbut, and M. M. Scherer, Abelian Higgs model at four loops, fixed-point collision and deconfined criticality, Phys. Rev. B **100**, 134507 (2019).

[66] C. Bonati, A. Pelissetto, and E. Vicari, Phase diagram, symmetry breaking, and critical behavior of three-Dimensional lattice multiflavor scalar chromodynamics, Phys. Rev. Lett. **123**, 232002 (2019); Three-dimensional lattice multiflavor scalar chromodynamics: Interplay between global and gauge symmetries, Phys. Rev. D **101**, 034505 (2020).

[67] S. Sachdev, H. D. Scammell, M. S. Scheurer, and G. Tarnopolsky, Gauge theory for the cuprates near optimal doping, Phys. Rev. B **99**, 054516 (2019).

[68] G.-Y. Zhu and G.-M. Zhang, Gapless Coulomb state emerging from a self-dual topological tensor-network state, Phys. Rev. Lett. **122**, 176401 (2019).

[69] C. Bonati, A. Pelissetto, and E. Vicari, Three-dimensional phase transitions in multiflavor scalar SO(N_c) gauge theories, Phys. Rev. E **101**, 062105 (2020).

[70] H. D. Scammell, K. Patekar, M. S. Scheurer, and S. Sachdev, Phases of SU(2) gauge theory with multiple adjoint Higgs fields in 2+1 dimensions, Phys. Rev. B 101, 205124 (2020)

[71] C. Bonati, A. Pelissetto and E. Vicari, Breaking of Gauge Symmetry in Lattice Gauge Theories, Phys. Rev. Lett. **127**, 091601 (2021)

[72] D. Weston and E. Babaev, Composite order in SU(N) theories coupled to an Abelian gauge field, Phys. Rev. B **104**, 075116 (2021).

[73] C. Bonati, A. Franchi, A. Pelissetto, and E. Vicari, Phase diagram and Higgs phases of 3D lattice SU(N_c) gauge theories with multiparameter scalar potentials, Phys. Rev. E **104**, 064111 (2021).

[74] A. Somoza, P. Serna, and A. Nahum, Self-dual criticality in three-dimensional $\mathbb{Z}_2$ gauge theory with matter, Phys. Rev. X **11**, 041008 (2021).

[75] C. Bonati, A. Pelissetto and E. Vicari, Lattice gauge theories in the presence of a linear gauge-symmetry breaking, Phys. Rev. E **104**, 014140 (2021).

[76] C. Bonati, A. Pelissetto, and E. Vicari, Critical behaviors of lattice U(1) gauge models and three-dimensional Abelian-Higgs gauge field theory, Phys. Rev. B **105**, 085112 (2022).

[77] C. Bonati, A. Pelissetto, and E. Vicari, Multicritical point of the three-dimensional Z_2 gauge Higgs model, Phys. Rev. B **105**, 165138 (2022).

[78] C. Bonati, A. Pelissetto, and E. Vicari, Scalar gauge-Higgs models with discrete Abelian symmetry group, Phys. Rev. E **105**, 054132 (2022)

[79] G. Bracci-Testasecca and A. Pelissetto, Multicomponent gauge-Higgs models with discrete Abelian gauge groups, J. Stat. Mech. 2304, 043101 (2023).

[80] C. Bonati, A. Pelissetto, and E. Vicari, Coulomb-Higgs phase transition of three-dimensional lattice Abelian Higgs gauge models with noncompact gauge variables and gauge fixing Phys. Rev. E **108**, 044125 (2023).

[81] T. Senthil, Deconfined quantum critical points: a review, in *50 years of the renormalization group*, dedicated to the memory of Michael E. Fisher, edited by Amnon Aharony, Ora Entin-Wohlman, David Huse, and Leo Radzihovsky, World Scientific arXiv:2306.12638

[82] M. Song, J. Zhao, L. Janssen, M. M. Scherer, and Z. Y. Meng, Deconfined quantum criticality lost, arXiv:2307.02547.

[83] C. Bonati, A. Pelissetto, and E. Vicari, Abelian Higgs gauge theories with multicomponent scalar fields and multiparameter scalar potentials, Phys. Rev. B **108**, 245154 (2023).

[84] C. Bonati, A. Pelissetto, and E. Vicari, Diverse universality classes of the topological deconfinement transitions of three-dimensional noncompact lattice Abelian-Higgs models, Phys. Rev. D **109**, 034517 (2024).

[85] C. Bonati, A. Pelissetto, and E. Vicari, Deconfinement transitions in three-dimensional compact lattice Abelian Higgs models with multiple-charge scalar fields, Phys.

Rev. E in press, arXiv:2402.06374.
[86] C. Bonati, A. Pelissetto, and E. Vicari, Strong-coupling critical behavior in three-dimensional lattice Abelian gauge models with charged N-component scalar fields and $SO(N)$ symmetry, arXiv:2403.12758.
[87] C. Bonati, A. Pelissetto, and E. Vicari, Stochastic gauge fixing to uncover critical vector correlations in lattice $\mathbb{Z}_2$-gauge N-vector Higgs models, in preparation.
[88] L. Oppenheim, M. Koch-Janusz, S. Gazit, and Z. Ringel, Machine Learning the Operator Content of the Critical Self-Dual Ising-Higgs Gauge Model, arXiv:2311.17994.
[89] W.-T. Xu, F. Pollmann, and M. Knap, Critical behavior of the Fredenhagen-Marcu order parameter at topological phase transitions, arXiv:2402.00127.
[90] C. Bonati, A. Pelissetto, and E. Vicari, Comment on *Machine Learning the Operator Content of the Critical Self-Dual Ising-Higgs Gauge Model* arXiv:2311.17994v1, arXiv:2401.10563.
[91] C. Bonati, A. Pelissetto, and E. Vicari, Higher-charge three-dimensional compact lattice Abelian-Higgs models, Phys. Rev. E **102**, 062151 (2020).
[92] A. M. Ferrenberg, J. Xu, and D. P. Landau, Pushing the limits of Monte Carlo simulations for the three-dimensional Ising model, Phys. Rev. E **97**, 043301 (2018).
[93] A. Pelissetto and E. Vicari, Critical phenomena and renormalization group theory, Phys. Rep. **368**, 549 (2002).
[94] A. Pelissetto and E. Vicari, Multicomponent compact Abelian-Higgs lattice models, Phys. Rev. E **100**, 042134 (2019).
[95] M. Hasenbusch, Monte Carlo study of an improved clock model in three dimensions, Phys. Rev. B **100**, 224517 (2019).
[96] Y. Deng, H. W. J. Blöte, and M. P. Nightingale, Surface and bulk transitions in three-dimensional $O(n)$ models, Phys. Rev. E **72**, 016128 (2005).
[97] H. G. Ballesteros, L. A. Fernandez, V. Martin-Mayor, and A. Munoz Sudupe, Finite size effects on measures of critical exponents in $d = 3$ O(N) models, Phys. Lett. B **387**, 125 (1996).
[98] M. Hasenbusch, Three-dimensional O(N)-invariant φ^4 models at criticality for ≥ 4, Phys. Rev. B **105**, 054428 (2022).
[99] F. Delfino, A. Pelissetto, and E. Vicari, Three-Dimensional Antiferromagnetic CP^{N-1} Models, Phys. Rev. E **91** 052109 (2015).
[100] P. Butera and M. Comi, N-vector spin models on the sc and the bcc lattices: a study of the critical behavior of the susceptibility and of the correlation length by high temperature series extended to order β^{21}, Phys. Rev. B **56**, 8212 (1997).
[101] M. Campostrini, A. Pelissetto, P. Rossi, and E. Vicari, Four-point renormalized coupling in O(N) models, Nucl. Phys. B **459**, 207 (1996).
[102] M. Campostrini, M. Hasenbusch, A. Pelissetto, and E. Vicari, Theoretical estimates of the critical exponents of the superfluid transition in ^{4}He by lattice methods, Phys. Rev. B **74**, 144506 (2006).
[103] R. Guida and J. Zinn-Justin, Critical exponents of the N-vector model, J. Phys. A **31**, 8103 (1998).
[104] M. V. Kompaniets and E. Panzer, Minimally subtracted six-loop renormalization of ϕ^4-symmetric theory and critical exponents, Phys. Rev. D **96**, 036016 (2017).
[105] S. M. Chester, W. Landry, J. Liu, D. Poland, D. Simmons-Duffin, N. Su, and A. Vichi, Carving out OPE space and precise O(2) model critical exponents, J. High Energy Phys. **06**, 142 (2020).
[106] M. Hasenbusch and E. Vicari, Anisotropic perturbations in 3D O(N) vector models, Phys. Rev. B **84**, 125136 (2011).
[107] P. Calabrese, A. Pelissetto, and E. Vicari, Multicritical behavior of $\mathrm{O}(n_1) \oplus \mathrm{O}(n_2)$-symmetric systems, Phys. Rev. B **67**, 054505 (2003).
[108] P. Calabrese, A. Pelissetto, and E. Vicari, Critical structure factors of bilinear fields in $O(N)$ vector models, Phys. Rev. E **65**, 046115 (2002).
[109] A. Pelissetto and E. Vicari, Scaling behaviors at quantum and classical first-order transitions, in *50 years of the renormalization group*, chapter 27, dedicated to the memory of Michael E. Fisher, edited by A. Aharony, O. Entin-Wohlman, D. Huse, and L. Radzihovsky, World Scientific (2024). [arXiv:2302.08238]
[110] K.-S. Liu and M. E. Fisher, Quantum lattice gas and the existence of a supersolid, J. Low Temp. Phys. **10**, 655 (1972).
[111] M. E. Fisher and D. R. Nelson, Spin Flop, Supersolids, and Bicritical and Tetracritical Points, Phys. Rev. Lett. **32**, 1350 (1974).
[112] D. R. Nelson, J. M. Kosterlitz, and M. E. Fisher, Renormalization-Group Analysis of Bicritical and Tetracritical Points Phys. Rev. Lett. **33**, 813 (1974); J. M. Kosterlitz, D. R. Nelson, and M. E. Fisher, Bicritical and tetracritical points in anisotropic antiferromagnetic systems, Phys. Rev. B **13**, 412 (1976).
[113] A. Kudlis, A. Aharony, and O. Entin-Wohlman, Effective exponents near bicritical points, To appear in Proc. FQMT, EPJ ST., arXiv:2304.08265.
[114] A. Aharony, 50 years of correlations with Michael Fisher and the renormalization group, in *50 years of the renormalization group*, dedicated to the memory of Michael E. Fisher, edited by A. Aharony, O. Entin-Wohlman, D. Huse, and L. Radzihovsky, World Scientific (2024). [arXiv:2305.13940]
[115] S. F. Edwards and P. W. Anderson, Theory of spin glasses, J. Phys. F: Met. Phys. **5**, 965 (1975).
[116] M. Hasenbusch, F. Parisen Toldin, A. Pelissetto, and E. Vicari, The critical behavior of the 3D $\pm J$ Ising model at the ferromagnetic transition line, Phys. Rev. B **76**, 094402 (2007); Magnetic-glassy multicritical behavior of 3D $\pm J$ Ising model, Phys. Rev. B **76**, 184202 (2007).
[117] M. Hasenbusch, A. Pelissetto, and E. Vicari, Critical behavior of three-dimensional Ising spin glass models, Phys. Rev. B **78**, 214205 (2008); G. Ceccarelli, A. Pelissetto, and E. Vicari, Ferromagnetic-glassy transitions in three-dimensional Ising spin glasses, Phys. Rev. B **84**, 134202 (2011).
[118] A. G. Cavaliere and A. Pelissetto, Disordered Ising model with correlated frustration, J. Phys. A: Math. Theor. **52**, 174002 (2019).